Chemical Engineering Journal 284 (2016) 260–269

Contents lists available at ScienceDirect

Chemical Engineering Journal

journal homepage: www.elsevier.com/locate/cej

Novel efficient process for methanol synthesis by CO_2 hydrogenation

Anton A. Kiss [a,b,*], J.J. Pragt [a], H.J. Vos [a], G. Bargeman [a], M.T. de Groot [c]

[a] AkzoNobel – Research, Development & Innovation, Process Technology SRG, Zutphenseweg 10, 7418 AJ Deventer, The Netherlands
[b] Sustainable Process Technology Group, Faculty of Science and Technology, University of Twente, PO Box 217, 7500 AE Enschede, The Netherlands
[c] AkzoNobel, Industrial Chemicals, Competence Team Technology, Stationsstraat 77, 3800 AE Amersfoort, The Netherlands

HIGHLIGHTS

- Efficient process for methanol synthesis by hydrogenation of carbon dioxide.
- Stripping of products with wet hydrogen for double positive effect.
- Minimum consumption of raw materials, and limited use of electricity and steam.

ARTICLE INFO

Article history:
Received 29 May 2015
Received in revised form 10 August 2015
Accepted 11 August 2015
Available online 1 September 2015

Keywords:
CO_2 hydrogenation
Low-pressure process
Cu/Zn catalyst
H_2 stripping
Energy efficiency

ABSTRACT

Methanol is an alternative fuel that offers a convenient solution for efficient energy storage. Complementary to carbon capture activities, significant effort is devoted to the development of technologies for methanol synthesis by hydrogenation of carbon dioxide. While CO_2 is available from plenty of sources, cheap sources of H_2 are less frequently found. An additional source of hydrogen at industrial scale is the wet hydrogen by-product of chlorine production.

This study is the first to propose an efficient process for methanol synthesis by CO_2 hydrogenation using wet hydrogen by-product from chlor-alkali production. A key feature of this novel process is the use of a stripping unit where the wet hydrogen flows in counter-current mode with the condensed methanol–water mixture resulting from the high-pressure low-temperature separator after the reaction. This operation has a double positive effect, as it removes the CO/CO_2 from the methanol–water mixture thus allowing a complete recycle of CO_2 and avoiding its presence in the product, while also removing the water from the wet hydrogen thus avoiding the negative impact of adding water on the equilibrium conversion – with consumption figures of 550 kWh electricity and 0.48–1.16 ton steam per ton methanol.

1. Introduction

Methanol is a viable alternative energy source, offering a convenient solution for the efficient energy storage on a large scale, while playing an important role in economy and sustainability by converting the CO_2 waste from industry into a valuable product [18]. At industrial scale, methanol is produced from synthesis gas ($CO/CO_2/H_2$) using various catalysts based on $CuO/ZnO/Al_2O_3$ [1]. Complementary to carbon capture and sequestration (CCS), much effort is being put on the development of technologies for methanol production from carbon dioxide. Several review papers published during the past decade cover this topic very well.

Liu et al. [17] reviewed the progress in the catalyst innovation, optimization of the reaction conditions, reaction mechanism, and catalyst performance in CO and CO_2 hydrogenation to methanol, highlighting the key issues of catalyst improvement and areas of priority in R&D.

Centi and Perathoner [4] analyzed the possibilities of converting CO_2 to fuels, noting that the requisites for this objective are: minimization of the consumption of hydrogen (sources), production of fuels that can be easily stored and transported, and the use of renewable energy sources. Their review included CO_2 reverse water–gas shift (WGS) and hydro-genation to hydrocarbons, alcohols, dimethyl ether or formic acid, as well as the reaction to synthesis gas; photo- and electrochemical/catalytic conversion; and thermo-chemical conversion.

Kondratenko et al. [15] discussed the heterogeneously catalyzed hydrogenation, as well as the photocatalytic and electrocatalytic conversion of CO_2 to hydrocarbons or oxygenates, along with the design of electrodes to improve their performance

Abbreviations: SN, stoichiometric number; WGS, water-gas shift reaction.

* Corresponding author at: AkzoNobel – Research, Development & Innovation, Process Technology SRG, Zutphenseweg 10, 7418 AJ Deventer, The Netherlands. Tel.: +31 26 366 9420.
E-mail address: TonyKiss@gmail.com (A.A. Kiss).

http://dx.doi.org/10.1016/j.cej.2015.08.101
1385-8947/

Nomenclature

Notation

A	pre-exponential factor
c	concentration (mol/kg)
f	fugacity (bar *or* Pa)
GHSV	gas hourly space velocity (m^3/kg_{cat} h)
k	reaction rate constant
K_R	equilibrium constant of reaction R
K_i	adsorption constant of component i (1/bar)
m	number of parameters (–)
p	pressure (bar)
R	gas constant = 8.314 (J/mol K)
W	weight of catalyst (kg)
y_i	gas mol fraction of component i (–)

Greek symbols

ΔH	enthalpy change (kJ/mol)
ΔS	entropy change (kJ/mol K)
θ_{CO}	Langmuir adsorption term CO
θ_{CO_2}	Langmuir adsorption term CO_2
θ_i	fractional occupation of s1-sites with species i
λ_j	fractional occupation of s2-sites with species j
λ_H	Langmuir adsorption term for dissociated hydrogen

Subscripts

i	component i (e.g. CO, CO_2, H_2, CH_3OH, H_2O)

and the recent developments of the application of ionic liquids as electrolytes and of microorganisms as co-catalysts.

Saeidi et al. [19] focused on hydrocarbon and methanol synthesis as methods to convert CO_2 to value-added products. The reaction mechanisms as well as the effects of catalyst, reactor type and operating conditions on product efficiency enhancement of each process were reviewed. Also a brief overview on the reactor types and configurations was provided.

Yan et al. [21] concentrated on the recent advances in designing efficient catalysts for the hydrogenation of CO_2 to fuels, e.g. CO_2 hydrogenation to methanol, CO_2 conversion to CO via reverse WGS reaction and production of hydrocarbons through Fischer–Tropsch synthesis.

Jadhav et al. [10] tackled various aspects on the CO_2 hydrogenation reaction system such as: thermodynamics, innovations in catalysts, influences of reaction variables, overall catalyst performance, reaction mechanism and kinetics, and recent technological advances.

Ali et al. [1] made a critical review on innovative catalysts for methanol synthesis, the research progress for their development and their use in the catalytic process, while providing an overview on recent developments in methanol synthesis from syngas, CO_2 hydrogenation and photo-catalytic reduction of CO_2. The use of various reactors, the influence of preparation method, support, promoter, different types of catalysts used, their properties and performance during methanol synthesis were also thoroughly reviewed.

While plenty of CO_2 is available from CCS activities, flue gas or as by-product in various processes (e.g. bioethanol production), the sources of hydrogen are more limited but feature processes such as steam methane reforming, coal gasification, partial oxidation of light oil residues, dry reforming, water electrolysis, sulfur-iodine or copper chloride processes [10]. Another major industrial source is the chlor-alkali process, where H_2 is formed as by-product of the salt electrolysis. Based on stoichiometry, 1 ton of chlorine leads to 28 kg hydrogen that can be further converted into 149 kg methanol, using 205 kg CO_2.

This article is the first to propose an efficient process for the CO_2 conversion to methanol using wet hydrogen (saturated with water) from brine electrolysis, in a catalytic process based on highly active Cu/Zn/Al/Zr fibrous catalyst [14]. For convenience, the results are provided for a 100 ktpy methanol plant, rigorously simulated in Aspen Plus and including experimental data previously reported in literature [2].

2. Problem statement

Methanol synthesis requires efficient chemical processes and inexpensive raw materials. Converting carbon dioxide to methanol by hydrogenation is considered to be a great industrial opportunity [18]. While cheap CO_2 is available from many sources, the options for low-cost hydrogen are rather limited. An interesting option is the use of wet hydrogen available as by-product in the chlor-alkali production. The issue is that the direct use of water saturated hydrogen stream has a strong negative impact on the chemical equilibrium. To solve this issue, an efficient process is proposed that includes a key feature – namely the use of stripper that has a double positive effect as it removes the CO_2 from the methanol–water mixture produced and avoids the presence of CO/CO_2 in the products, while also removing the water from the wet hydrogen feed initially saturated with water. The efficiency of the process is thus increased, leading to low consumption figures.

3. Process simulation

This section presents the main results for a plant producing 100 ktpy methanol, by CO_2 hydrogenation using a highly active Cu/Zn/Al/Zr fibrous catalyst [2].

3.1. Property model

The complete process was rigorously simulated in Aspen Plus using the RK-Soave property model which is most suitable for these components (H_2, CO, CO_2, H_2O, and CH_3OH) and conditions (pressure up to 50 bar and temperature up to 250 °C). The non-random two-liquid (NRTL) model was used complementary to the RK-Soave property model, for modeling the distillation section operating at low pressure and in which no hydrogen is present. This is in line with literature recommendations for such systems [12,6]. Note that all the binary interaction parameters related to the property models RK-Soave and NRTL are available in the pure components databank of the Aspen Plus process simulator.

3.2. Chemical reactions

The pathways for methanol formation from CO_2/CO and H_2 on a metallic Cu catalyst are given in Kondratenko et al. [15]. The actual chemistry of CO_2 hydrogenation involves three main equilibrium reactions (A, B and C) leading to methanol and water [7]:

$$\text{A)}\ CO + 2H_2 \leftrightarrows CH_3OH \quad \Delta H_{298K} = -90.77\text{kJ/mol} \tag{1}$$

$$\text{B)}\ CO_2 + H_2 \leftrightarrows CO + H_2O \quad \Delta H_{298K} = +41.21\text{kJ/mol, Reverse WGS reaction} \tag{2}$$

$$\text{C)}\ CO_2 + 3H_2 \leftrightarrows CH_3OH + H_2O \quad \Delta H_{298K} = -49.16\text{kJ/mol} \tag{3}$$

The CO_2 conversion to CO (reaction B) is endothermic hence the temperature increase is favorable to the equilibrium. However, the CO and CO_2 conversions to methanol (reactions A and C) are exothermic hence the temperature increase has a negative impact

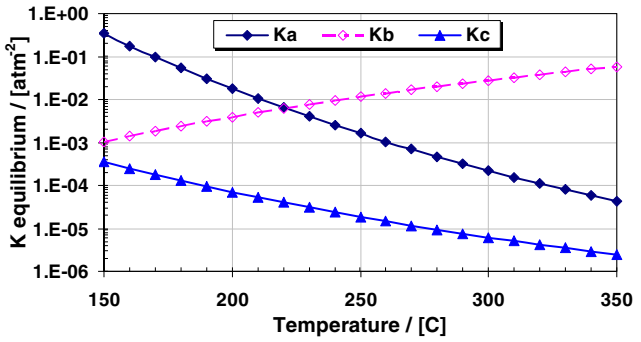

Fig. 1. Effect of temperature on the equilibrium constants of the main chemical reactions.

on equilibrium. Thus, higher methanol yields are obtained at lower temperatures and higher pressures. This effect is clearly illustrated in Fig. 1 showing the effect of temperature on equilibrium.

Note that in a process having all three components (CO_2, CO, and H_2) in the feed, the mole fractions have to be adjusted such that the optimal stoichiometric number (SN) is equal to 2. A higher value (SN > 2) indicates that there is an excess of H_2 in the feed gas, while a lower value (SN < 2) means that there is an excess of carbon. When only CO_2 and H_2 are present in the feed, a H_2:CO_2 ratio of 3:1 ensures that SN = 2. The SN number is calculated as follows:

$$SN = \frac{y_{H_2} - y_{CO_2}}{y_{CO} + y_{CO_2}} \tag{4}$$

3.3. Chemical equilibrium

The values for the equilibrium constants (K_A, K_B and K_C) were reported by Lim et al. [16], using R = 8.314 J/mol K and K_i. Note that the study of Lim et al. [16] used the experimental data from Graaf et al. [8], so basically it is the same data but provided in an explicit model which provides a consistent framework for process simulations in Aspen Plus.

The comparison between the data from literature [16] and the equilibrium constant values evaluated within Aspen Plus using the equilibrium reactor showed an excellent agreement. Note that in Aspen Plus, the equilibrium constants are evaluated based upon fugacity in [atm]. A conversion was made to [Pa] based correlations as those will be required to express the driving force term of the kinetic rate equations:

$$\ln K_A = \frac{9.8438\times10^4}{RT} - 29.07 \rightarrow K_A = 2.3717\times10^{-13}\exp\left(\frac{9.8438\times10^4}{RT}\right)\ [\text{atm}^{-2}]$$
$$\ln K_A = -52.096 + \frac{11840}{T} \quad \text{with } K_A\ [\text{Pa}^{-2}] \tag{5}$$

$$\ln K_B = \frac{-4.3939\times10^4}{RT} + 5.639 \rightarrow K_B = 2.8118\times10^{2}\exp\left(\frac{-4.3939\times10^4}{RT}\right)\ [-]$$
$$\ln K_B = 5.639 + \frac{-5285}{T} \quad \text{with } K_B\ [-] \tag{6}$$

$$K_C = K_A \times K_B \qquad \rightarrow K_C = 6.6688\times10^{-11}\exp\left(\frac{5.4499\times10^4}{RT}\right)\ [\text{atm}^{-2}]$$
$$\ln K_C = -46.457 + \frac{6555}{T} \qquad \text{with } K_C\ [\text{Pa}^{-2}] \tag{7}$$

3.4. Catalyst and kinetics

Many catalysts are available for CO_2 hydrogenation, based on Cu/Zn formulations [21]. Also most of the commercial catalysts available from several catalyst manufacturers (e.g. Katalko from Johnson-Matthey, MegaMax from Clariant) have high performance. In this work, the kinetic model A3B2C3 – which was shown to be the best kinetic model out of the 48 models tested by Graaf et al. [9] – combined with kinetic data from An et al. [2] was implemented in Aspen Plus. Note that other adequate kinetic models are also available in the literature [3,20,5]; and numerous publications from Haldor Topsoe.

The experimental data from An et al. [2] validates the model of Graaf et al. [9] and it was obtained for a fibrous Cu/Zn/Al/Zr catalyst that was designed especially for the hydrogenation of CO_2. Note that the Langmuir–Hinshelwood kinetic model assumes two different active sites. CO and CO_2 absorb competitively on the so called s1-sites, while H_2 and H_2O are absorbed competitively on the s2-sites. According to Graaf et al. [9] the adsorption of methanol is assumed to be negligible, while H_2 is believed to adsorb dissociatively – hence the use of λ_H term. Nonetheless, it is rather straightforward to derive alternative kinetic rate expressions that are based on the molecular adsorption of H_2. The elementary reactions are described as follows [9]:

Adsorption equilibria

$$CO + s1 = COs1 \tag{8}$$

$$CO_2 + s1 = CO_2s1 \tag{9}$$

$$H_2 + 2s2 = 2Hs2 \tag{10}$$

$$H_2O + s2 = H_2Os2 \tag{11}$$

Reaction (A)

$$\text{(A1)}\quad COs1 + Hs2 = HCOs1 + s2 \tag{12}$$

$$\text{(A2)}\quad HCOs1 + Hs2 = H_2COs1 + s2 \tag{13}$$

$$\text{(A3)}\quad H_2COs1 + Hs2 = H_3COs1 + s2 \tag{14}$$

$$\text{(A4)}\quad H_3COs1 + Hs2 = CH_3OH + s1 + s2. \tag{15}$$

Reaction (B)

$$\text{(B1)}\quad CO_2s1 + Hs2 = HCO_2s1 + s2 \tag{16}$$

$$\text{(B2)}\quad HCO_2s1 + Hs2 = COs1 + H_2Os2. \tag{17}$$

Reaction (C)

$$\text{(C1)}\quad CO_2s1 + Hs2 = HCO_2s1 + s2 \tag{18}$$

$$\text{(C2)}\quad HCO_2s1 + Hs2 = H_2CO_2s1 + s2 \tag{19}$$

$$\text{(C3)}\quad H_2CO_2s1 + Hs2 = H_3CO_2s1 + s2 \tag{20}$$

$$\text{(C4)}\quad H_3CO_2s1 + Hs2 = H_2COs1 + H_2Os2 \tag{21}$$

$$\text{(C5)}\quad H_2COs1 + Hs2 = H_3COs1 + s2 \tag{22}$$

$$\text{(C6)}\quad H_3COs1 + Hs2 = CH_3OH + s1 + s2. \tag{23}$$

In case of the best model concluded by Graaf et al. [9] the rate controlling steps for each overall reaction A, B and C are A3, B2, and C3 respectively – hence the notation A3B2C3.

The corresponding rate equations for the kinetic model A3B2C3 are:

$$r_{CH_3OH,A3} = k_A \frac{K_{CO}\left[f_{CO}f_{H_2}^{3/2} - f_{CH_3OH}/(K_A\sqrt{f_{H_2}})\right]}{(1 + K_{CO}f_{CO} + K_{CO_2}f_{CO_2})[\sqrt{f_{H_2}} + (K_{H_2O}/\sqrt{K_H})f_{H_2O}]} \tag{24}$$

$$r_{CO,B2} = r_{H_2O,B2} = k_B \frac{K_{CO_2}[f_{CO_2}f_{H_2} - f_{H_2O}f_{CO}/K_B]}{(1 + K_{CO}f_{CO} + K_{CO_2}f_{CO_2})\left[\sqrt{f_{H_2}} + (K_{H_2O}/\sqrt{K_H})f_{H_2O}\right]} \tag{25}$$

$$r_{CH_3OH,C3} = r_{H_2O,C3} = k_C \frac{K_{CO_2}\left[f_{CO_2} f_{H_2}^{3/2} - f_{H_2O} f_{CH_3OH}/(f_{H_2}^{3/2} K_C)\right]}{(1 + K_{CO} f_{CO} + K_{CO_2} f_{CO_2})[\sqrt{f_{H_2}} + (K_{H_2O}/\sqrt{K_H}) f_{H_2O}]} \quad (26)$$

For example, the origin of $r_{CH_3OH,A3}$ is explained hereafter.

$$r_{A3+} = k_{A3+} \theta_{H_2CO} \lambda_H \quad (27)$$

$$K_{A1} = \frac{\theta_{HCO}}{\theta_{CO}} \cdot \frac{\lambda_e}{\lambda_H} = \frac{\theta_{HCO}}{\theta_{CO}} \cdot \frac{1}{\sqrt{K_H f_{H_2}}} \text{ and } K_{A2} = \frac{\theta_{H_2CO}}{\theta_{HCO}} \cdot \frac{\lambda_e}{\lambda_H} = \frac{\theta_{H_2CO}}{\theta_{HCO}} \cdot \frac{1}{\sqrt{K_H f_{H_2}}} \quad (28)$$

Therefore:

$$\theta_{H_2CO} = K_{A1} K_{A2} \left(\frac{\lambda_H}{\lambda_e}\right)^2 \theta_{CO} = K_{A1} K_{A2} K_H f_{H_2} \theta_{CO} \quad (29)$$

$$r_{A3+} = k_{A3+} K_{A1} K_{A2} K_H f_{H_2} \theta_{CO} \lambda_H \quad (30)$$

$$r_{A3+} = k_{A3+} K_{A1} K_{A2} \times \frac{K_{CO} f_{CO} (K_H f_{H_2})^{3/2}}{(1 + K_{CO} f_{CO} + K_{CO_2} f_{CO_2})(1 + \sqrt{K_H f_{H_2}} + K_{H_2O} f_{H_2O})} \quad (31)$$

The equilibrium constant of the overall reaction (A) is used to define the driving force term:

$$K_A = \frac{f_{CH_3OH}}{f_{CO} f_{H_2}^2} \rightarrow \text{Driving force} = f_{CO} f_{H_2}^{3/2} - f_{CH_3OH}/(K_A \sqrt{f_{H_2}}) \quad (32)$$

As a result it follows that:

$$r_A = r_{A3+} - r_{A3-} = k_{A3+} K_{A1} K_{A2} \frac{K_{CO} K_H^{3/2} \left(f_{CO} f_{H_2}^{3/2} - f_{CH_3OH}/(K_A \sqrt{f_{H_2}})\right)}{(1 + K_{CO} f_{CO} + K_{CO_2} f_{CO_2})(1 + \sqrt{K_H f_{H_2}} + K_{H_2O} f_{H_2O})} \quad (33)$$

According to Graaf et al. [9] it holds:

$$1 << \sqrt{K_H f_{H_2}} + K_{H_2O} f_{H_2O} \quad (34)$$

Thus:

$$r_A = k_{A3+} K_{A1} K_{A2} \frac{K_{CO} K_H \left(f_{CO} f_{H_2}^{3/2} - f_{CH_3OH}/(K_A \sqrt{f_{H_2}})\right)}{(1 + K_{CO} f_{CO} + K_{CO_2} f_{CO_2})\left(\sqrt{f_{H_2}} + (K_{H_2O}/\sqrt{K_H}) f_{H_2O}\right)} \quad (35)$$

Comparing this with the result presented by Eq. (43) in Graaf et al. [9], it is concluded that:

$$k_A = k_{A3+} K_{A1} K_{A2} K_H \quad (36)$$

The origin of the other terms ($r_{CO,B2}$ and $r_{CH3OH,C3}$) can be explained in a similar way.

The generalized rate expression to be used in Aspen Plus is given by:

$$r = \frac{(\text{kinetic factor})(\text{driving force expression})}{(\text{adsorption term})} \quad (37)$$

When a reference temperature T_o is not specified, the kinetic factor in Aspen is expressed by a pre-exponential factor and an Arrhenius term: kinetic factor $= kT^n \exp(-E_a/RT)$. All the required input data for the kinetic factor are included in Table 1 [2]. Note that the units for the pre-exponential constant depend on the units of the driving force term and the adsorption term. Therefore the units are not the same for all of the reactions.

The driving force expressions are as follows:

$$\text{Reaction A}: K_{CO} f_{CO} f_{H_2}^{3/2} - \frac{K_{CO}}{K_A} f_{CH_3OH} f_{H_2}^{-1/2} \ [\text{Pa}^{3/2}] \quad (38)$$

$$\text{Reaction B}: K_{CO_2} f_{CO_2} f_{H_2} - \frac{K_{CO_2}}{K_B} f_{H_2O} f_{CO} \ [\text{Pa}] \quad (39)$$

$$\text{Reaction C}: K_{CO_2} f_{CO_2} f_{H_2}^{3/2} - \frac{K_{CO_2}}{K_C} f_{H_2O} f_{CH_3OH} f_{H_2}^{-3/2} \ [\text{Pa}^{3/2}] \quad (40)$$

It should be noted that in Aspen Plus, the driving force is expressed in a generalized form:

$$K_1 \left(\prod c_i^{\nu_i}\right) - K_2 \left(\prod c_j^{\nu_j}\right) \quad (41)$$

When selecting the vapor phase as the reactive phase, and neglecting the difference between partial pressure and fugacity (i.e. assuming ideal gas), the partial pressures are used for the concentration. The resulting values for K_1 and K_2 are given in Table 2. In Aspen Plus, K_1 and K_2 are expressed in a logarithmic form, so the resulting input parameters are given in Table 3.

$$\ln(K) = A + \frac{B}{T} \quad (42)$$

The adsorption term is the same for all reactions. The expression applied in Aspen Plus is:

$$\left(\sum K_i [\prod c_j^{\nu_j}]\right)^m \quad (43)$$

Configuring Aspen Plus requires re-writing the adsorption term in the kinetic expression, which is the same for all three reactions [9]:

$$(1 + K_{CO} f_{CO} + K_{CO_2} f_{CO_2})(f_{H_2}^{1/2} + [K_{H_2O}/\sqrt{K_H}] f_{H_2O}) \ [bar^{1/2}] = \sqrt{f_{H_2}} + \frac{K_{H_2O}}{\sqrt{K_H}} f_{H_2O} + K_{CO} f_{CO} \sqrt{f_{H_2}} + \frac{K_{CO} K_{H_2O}}{\sqrt{K_H}} f_{CO} f_{H_2O} + K_{CO_2} f_{CO_2} \sqrt{f_{H_2}} + \frac{K_{CO_2} K_{H_2O}}{\sqrt{K_H}} f_{CO_2} f_{H_2O} \quad (44)$$

Table 1
Kinetic factor for reactions A, B and C (based on data from [2]) – the units used are [Pa] for fugacity and [mol/$g_{catalyst}$ s] = [kmol/$kg_{catalyst}$ s] for reaction rate.

Reaction	k	n	E_a [J/mol K]
A	4.0638×10^{-6} [kmol/kg_{cat} s Pa]	0	11,695
B	9.0421×10^{8} [kmol/kg_{cat} s $Pa^{1/2}$]	0	112,860
C	1.5188×10^{-33} [kmol/kg_{cat} s Pa]	0	266,010

Table 2
Constants for driving force (adsorption data from [2]); and chemical equilibrium data from [16].

Reaction	Expression K_1	K_1	Expression K_2	K_2
A	K_{CO} [Pa^{-1}]	8.3965×10^{-11} exp (118,270/RT)	K_{CO}/K_A [Pa]	3.5408×10^{12} exp (19,832/RT)
B	K_{CO_2} [Pa^{-1}]	1.7214×10^{-10} exp (81,287/RT)	K_{CO2}/K_B [Pa^{-1}]	6.1221×10^{-13} exp (125,226/RT)
C	K_{CO_2} [Pa^{-1}]	1.7214×10^{-10} exp (81,287/RT)	K_{CO2}/K_C [Pa]	2.5813×10^{10} exp (26,788/RT)

Table 3
Constants for driving force (from [2]) using the format for Aspen Plus.

	K_1		K_2	
Reaction	A	B	A	B
A	−23.20	14,225	28.895	2385
B	−22.48	9777	−28.12	15,062
C	−22.48	9777	23.974	3222

Table 4
K_i factors for adsorption term (terms 2, 3, 5 from [2]; rest is explicitly derived by calculation).

Term	Expression	a_i	b_i	$\prod c_j^{v_j}$
1	1	$a_1 = 1$	$b_1 = 0$	$\sqrt{f_{H_2}}$
2	$\frac{K_{H_2O}}{\sqrt{K_H}}$	$a_2 = 4.3676 \times 10^{-12}$	$b_2 = 1.1508 \times 10^5$	f_{H_2O}
3	K_{CO}	$a_3 = 8.3965 \times 10^{-11}$	$b_3 = 1.1827 \times 10^5$	$f_{CO}\sqrt{f_{H_2}}$
4	$\frac{K_{CO}K_{H_2O}}{\sqrt{K_H}}$	$a_4 = a_2 \times a_3$ $a_4 = 3.6673 \times 10^{-22}$	$b_4 = b_2 + b_3 = 2.3335 \times 10^5$	$f_{CO}f_{H_2O}$
5	K_{CO_2}	$a_5 = 1.7214 \times 10^{-10}$	$b_5 = 8.1287 \times 10^4$	$f_{CO_2}\sqrt{f_{H_2}}$
6	$\frac{K_{CO_2}K_{H_2O}}{\sqrt{K_H}}$	$a_6 = a_2 \times a_5$ $a_6 = 7.5184 \times 10^{-22}$	$b_6 = b_2 + b_5 = 1.9727 \times 10^5$	$f_{CO_2}f_{H_2O}$
		$A_i = \ln(a_i)$	$B_i = b_i/R$	$\prod c_j^{v_j}$
1	1	0	0	$\sqrt{f_{H_2}}$
2	$\frac{K_{H_2O}}{\sqrt{K_H}}$	−26.1568	13,842	f_{H_2O}
3	K_{CO}	−23.2006	14,225	$f_{CO}\sqrt{f_{H_2}}$
4	$\frac{K_{CO}K_{H_2O}}{\sqrt{K_H}}$	−49.3574	28,067	$f_{CO}f_{H_2O}$
5	K_{CO_2}	−22.4827	9777	$f_{CO_2}\sqrt{f_{H_2}}$
6	$\frac{K_{CO_2}K_{H_2O}}{\sqrt{K_H}}$	−48.6395	23,619	$f_{CO_2}f_{H_2O}$

Table 5
Comparison of experimental data from An et al. [2] with the results of the Aspen Plus calculations using LHHW kinetics.

SV = 6000 ml/g_{cat} h	CO_2 conversion		Methanol yield based on CO_2 feed	
T [K]	Experimental data[a]	Aspen Plus calculations	Experimental data[a]	Aspen Plus calculations
483	0.170	0.1244	0.110	0.1152
503	0.225	0.1957	0.155	0.1597
523	0.255	0.2398	0.178	0.1530
543	0.250	0.2404	0.140	0.1058
T = 523 K	CO_2 conversion		Methanol yield based on CO_2 feed	
SV [ml/$g_{catalyst}$ h]	Experimental data[b]	Aspen Plus calculations	Experimental data[b]	Aspen Plus calculations
1000	0.262	0.2428	0.193	0.1548
2000	0.260	0.2428	0.191	0.1548
4000	0.256	0.2421	0.180	0.1544
6000	0.250	0.2398	0.166	0.1530
8000	0.243	0.2362	0.153	0.1509
10,000	0.230	0.2321	0.134	0.1485

[a] Experimental data taken from Fig. 2 reported in An et al. [2].
[b] Experimental data taken from Fig. 4 reported in An et al. [2].

Both the numerator and the denominator of the kinetic rate equation are divided by $\sqrt{K_H}$ in order to reduce the number of variables since this allows lumping together K_H and K_{H2O}. Although the result is that the adsorption term is not dimensionless anymore, the result is mathematically the same for the reaction rate expression. This expression is the sum of 6 terms with the exponent $m = 1$. The combined K_i factors for each term are specified in Table 4. The adsorption constants are a function of temperature:

$$K_i = a_i \exp(b_i/RT) \tag{45}$$

Note that in Aspen Plus, K is expressed in a logarithmic form – for convenience, the resulting input parameters are also provided in Table 4.

$$\ln(K) = A + \frac{B}{T} \tag{46}$$

Finally, the LHHW-kinetics was configured in Aspen Plus and tested with a plug flow reactor (PFR) against equilibrium and kinetics data from literature [2]. An excess of catalyst was applied in order to reach the chemical equilibrium in the PFR. The comparison between the experimental and simulated data (illustrated in Table 5) shows a good agreement with less than 5% error around the operating process conditions, thus indicating a correct implementation of the kinetics. No model parameters were calculated and no changes were made to the kinetic data from An et al. [2] and the equilibrium data from Lim et al. [16] – based on the detailed model of Graaf et al. [8]. These were only translated from the implicit form to the explicit input format required by the process simulator Aspen Plus.

4. Results and discussion

4.1. Sensitivity analysis

Within Aspen Plus, the CO_2 converter was simulated by a plug-flow reactor (PFR) using the Soave-Redlich-Kwong EOS and NRTL with Henry components as property models. The amount of catalyst considered in the reactor corresponds to a gas hourly space velocity of GHSV = 5.9 m^3/kg_{cat} h. Due to the geometrical design of the multi-tubular reactor, the gas velocity does not exceed 1.5 m/s. The following parameters were varied in the specified range: T = 200–300 °C, p = 1–100 bar, reactants ratio $R = H_2$: CO_2 = 3–12, and catalyst loadings within the range GHSV = 0.1–10^5 m^3/kg_{cat} h. The following figures show the main results of the sensitivity analysis, in terms of methanol and CO yield as a function of temperature (Fig. 2 and Fig. 3), pressure (Fig. 4) and catalyst loading (Fig. 5), at different reactants ratios. Due to the kinetic limitations at lower temperatures versus equilibrium limitations at higher temperatures, an optimal operating region exists and this depends on the reactants ratio. The effect of pressure on the MeOH and CO yields is straightforward. The formation of methanol is clearly favored at higher pressures due to the fact that CO_2 and CO hydrogenation reactions proceed with a decrease of the total number of moles. Consequently, as more CO is converted to methanol at higher pressures, the CO yield decreases when the pressure is increased. Fig. 5 shows that at 200 °C the reaction is kinetically limited, as an increase in catalyst loading leads to an increase in methanol yield. Therefore, it makes sense to increase the catalytic activity at lower temperatures in order to improve the yield. However, at higher temperatures (>250 °C) the reaction is

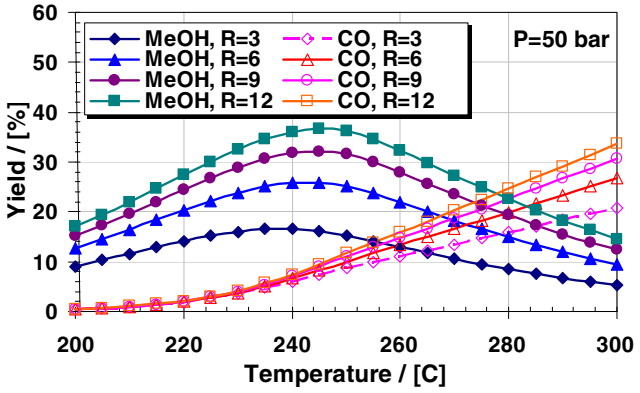

Fig. 2. Effect of temperature on the MeOH and CO yield, at fixed pressure and various reactants ratios (simulated results).

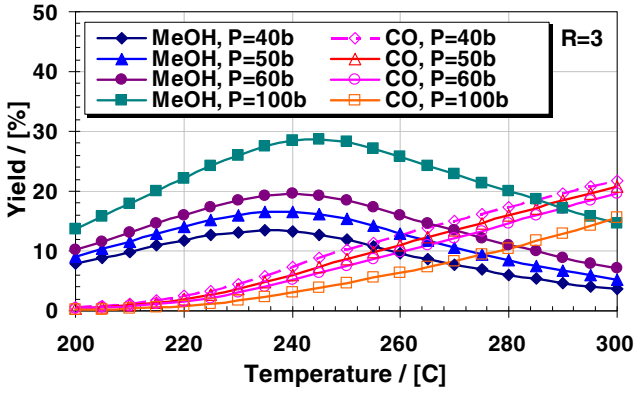

Fig. 3. Effect of temperature on the MeOH and CO yield, at fixed reactants ratio and various pressures (simulated results).

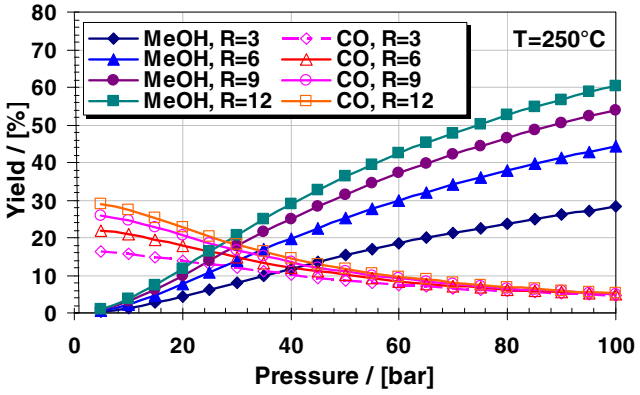

Fig. 4. Effect of pressure on the MeOH and CO yield, at fixed temperature and various reactants ratios (simulated results).

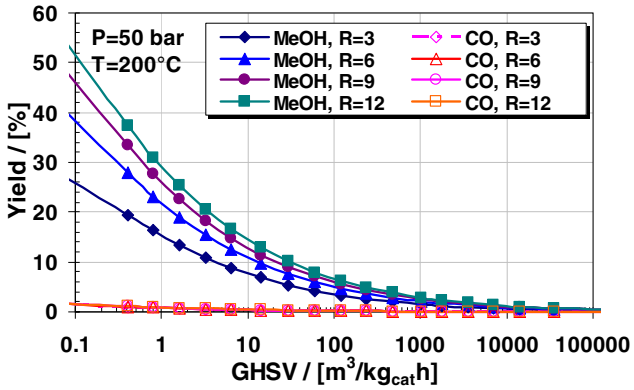

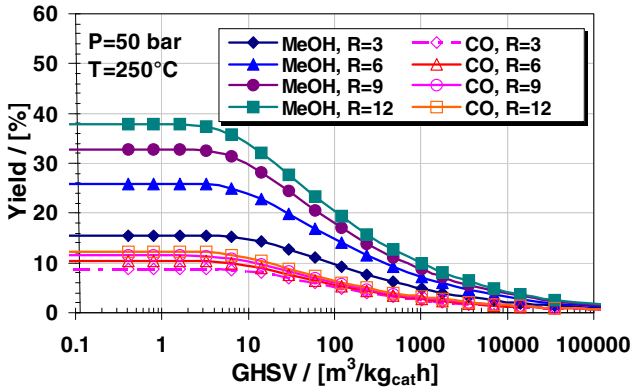

Fig. 5. Effect of the catalyst loading on the MeOH and CO yield (simulated results), at various reactants ratios and fixed pressure and temperature (p = 50 bar, T = 200 and T = 250 °C).

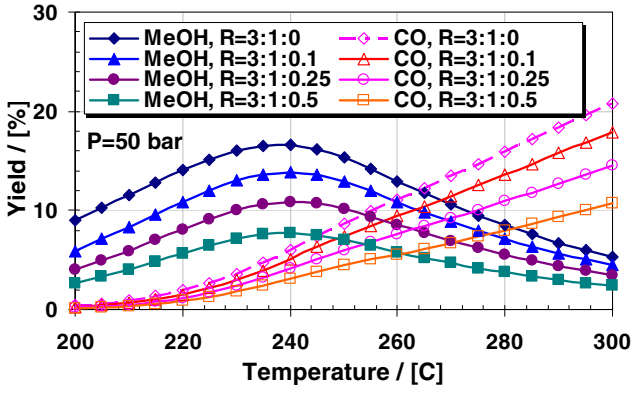

Fig. 6. Effect of water presence ($R = H_2:CO_2:H_2O$) on the MeOH and CO yield, at fixed pressure and along a temperature range (simulated results).

equilibrium limited when a sufficient amount of catalyst is used (GHSV < 10 m^3/kg_{cat} h), hence any further increase of the catalyst loading has no effect at all.

Furthermore, Fig. 6 shows the theoretical effect of water content in the reactor feed – more water leads to decreased performance as the presence of water has a detrimental effect on the equilibrium. However, it should be noted that in this new process the humidity (water content) of the hydrogen feed is not an actual variable, since the fresh feed stream is assumed to be saturated with water at ambient conditions hence this is the worst case scenario.

4.2. Process description

The classic low-pressure methanol process follows the generic scheme shown in Fig. 7 [7] – which is a typical reaction-separation-recycle system [11,13]. Basically, the reactants are brought to the required temperature and pressure then fed together (matching the stoichiometric number SN = 2) to a reactor operated at 200–300 °C and 50–100 bar. Due to the chemical equilibrium limitations, the conversion is incomplete so the reactor outlet will comprise of products (methanol and water) as well as unconverted reactants (CO*x* and hydrogen). This gaseous mixture is cooled and flashed to separate the condensable products from the non-condensable reactants, which are recycled. The condensed

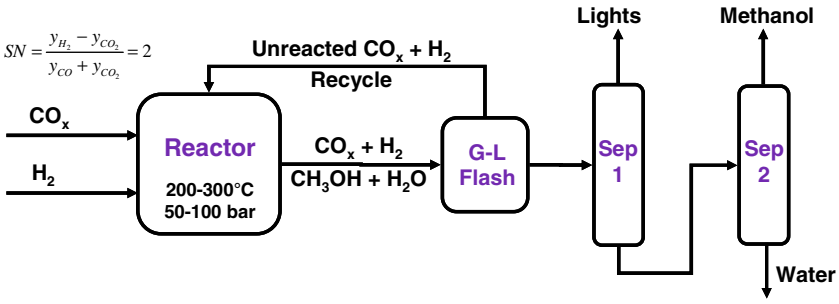

Fig. 7. Generic processing scheme for methanol synthesis from syngas or by CO_2 hydrogenation.

components are then separated in two steps, typically by a direct distillation sequence, into lights (dissolved CO*x* and minor light impurities), methanol and a water stream.

In this work, a plant capacity of 100 ktpy methanol is considered. Fig. 8 presents the proposed process flowsheet, while the complete mass and energy balance is provided in Table 6. Compared to the classic low-pressure methanol process reported [7] there are several key differences, described hereafter. The fresh CO_2 feed stream is mixed with the recycle gas stream and fed to the feed-effluent-heat-exchanger (FEHE) without decompression and heating. This leads to a lower gas flowrate to the recycle compressor (COMP2) and thus reduced requirements of electricity.

It is worth noting that using classic process synthesis heuristics we have also evaluated alternative process configurations that aimed to take advantage of having separate hydrogen and CO_2 feed streams (such as higher flexibility and methanol yield, lower energy requirements). However, no significant improvement was observed by feeding the reactants as mixed or pure components all at once or added along the catalytic reactor. The main reason is that the reactor outlet is in all cases close to the equilibrium hence implicitly limited. Consequently, the strategy of feeding the reactants has no effect on a reactor reaching 100% of the equilibrium conversion. The best alternative strategy was to feed the mixed reactants to the reactor working at lower end temperature, and to strip out the dissolved CO_2 from the methanol using the fresh feed of hydrogen that is then mixed with the CO_2 and the recycle stream. This strategy leads to the highest methanol yield and the lowest energy requirements per ton product. As shown later, this strategy is especially beneficial when wet fresh hydrogen is used, since the addition of wet fresh hydrogen does not only result in the stripping and recycling of CO_2 and CO from the produced methanol, but to removal of the water from the fresh hydrogen as well, thus leading to even larger improvements in CO_2 conversion per pass and energy reduction.

The fresh wet hydrogen feed from chlorine production by salt electrolysis is pressurized to 45 bar in a primary multi-stage compressor (COMP1). The hydrogen compressor (COMP1) was optimized (e.g. reducing the intermediate cooling temperature to less than 170 °C) to take advantage of the compression curve, and therefore further reduce the compression duty. The resulting gas mixture is heated up in a feed-effluent heat-exchanger (FEHE) by the reactor outlet stream, and then fed to a multi-tubular plug-flow reactor (PFR) operated isothermally at 50 bar and 250 °C. The heat of reaction generated in the reactor can be used to generate high pressure steam. The multi-tubular catalytic reactor has the following characteristics: 12 m length, 810 tubes of 0.06 m diameter, and a

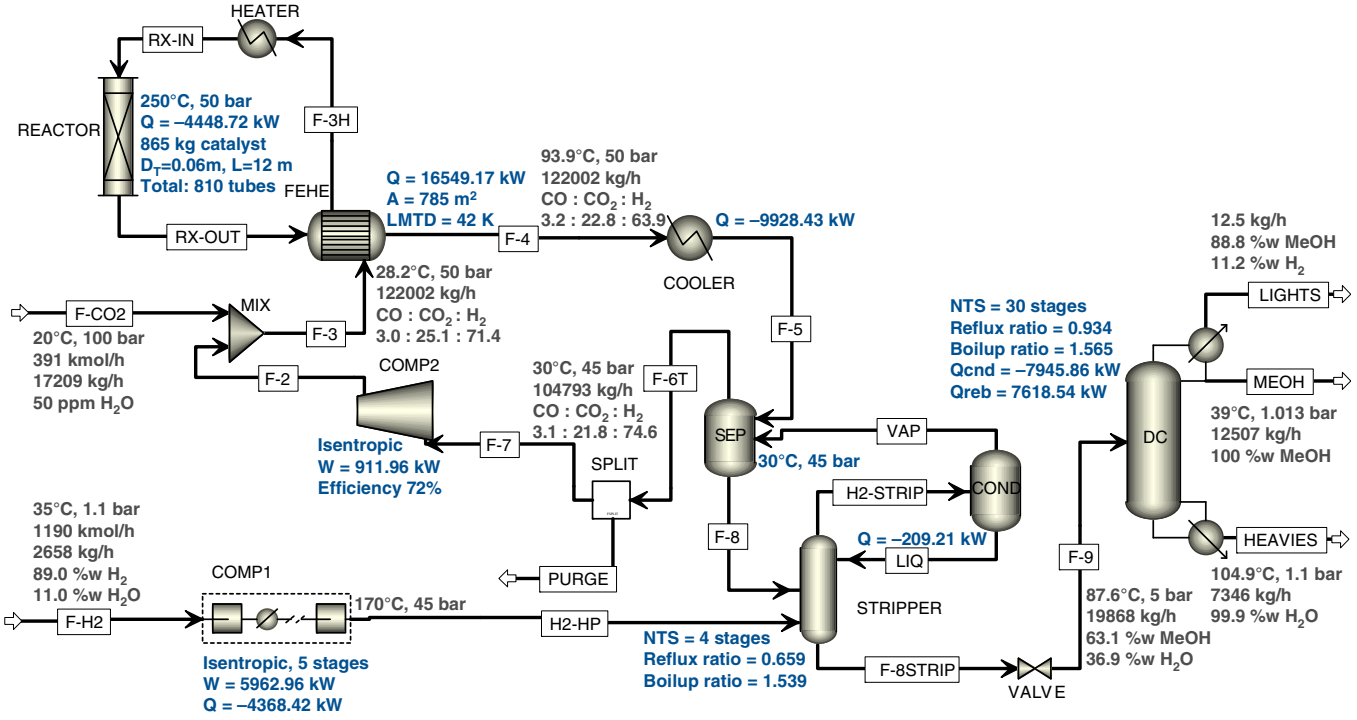

Fig. 8. Aspen Plus flowsheet of an efficient process for methanol synthesis by CO_2 hydrogenation.

Table 6
Mass and energy balance of the proposed process for methanol synthesis.

	F-2	F-3	F-3H	F-4	F-5	F-6T	F-7	F-8	F-8STRIP	F-9	F-CO_2
Temperature C	42.1	28.2	225.0	93.9	31.0	30.0	30.0	30.0	92.2	87.6	20.0
Pressure bar	50	50	50	50	50	45	45	45	45.2	5.066	100
Vapor frac	1	0.999	1	0.956	0.900	1	1	0	0	0.001	0
Mole flow kmol/h	8649.99	9041.05	9041.05	8259.03	8259.03	8650.00	8649.99	819.06	799.03	799.03	391.06
Mass flow kg/h	104793.54	122002.69	122002.69	122002.69	122002.69	104793.65	104793.54	21104.88	19867.90	19867.90	17209.15
Volume flow cum/h	4608.29	4572.55	7644.01	4878.20	3822.70	4907.32	4907.32	24.62	25.79	31.68	22.05
Enthalpy gcal/h	−185.29	−223.12	−208.89	−226.94	−235.48	−186.07	−186.07	−52.50	−49.30	−49.30	−37.83
Mass flow kg/h											
CO	7492.57	7492.57	7492.57	7492.57	7492.57	7492.57	7492.57	2.11	0.00	0.00	0.00
CO_2	82810.65	100018.93	100018.93	82810.73	82810.73	82810.73	82810.65	1344.24	0.00	0.00	17208.28
H_2	13011.73	13011.73	13011.73	10647.05	10647.05	13011.74	13011.73	1.30	1.45	1.45	0.00
H_2O	3.94	4.80	4.80	7048.93	7048.93	3.94	3.94	7045.40	7337.72	7337.72	0.86
CH_3OH	1474.66	1474.66	1474.66	14003.40	14003.40	1474.66	1474.66	12711.83	12528.74	12528.74	0.00
Mass frac CO	0.0715	0.0614	0.0614	0.0614	0.0614	0.0715	0.0715	0.0001	0.0000	0.0000	0.0000
Mass frac CO_2	0.7902	0.8198	0.8198	0.6788	0.6788	0.7902	0.7902	0.0637	0.0000	0.0000	1.0000
Mass frac H_2	0.1242	0.1067	0.1067	0.0873	0.0873	0.1242	0.1242	0.0001	0.0001	0.0001	0.0000
Mass frac H_2O	0.0000	0.0000	0.0000	0.0578	0.0578	0.0000	0.0000	0.3338	0.3693	0.3693	0.0001
Mass frac CH_3OH	0.0141	0.0121	0.0121	0.1148	0.1148	0.0141	0.0141	0.6023	0.6306	0.6306	0.0000
Mole frac CO	0.0309	0.0296	0.0296	0.0324	0.0324	0.0309	0.0309	0.0001	0.0000	0.0000	0.0000
Mole frac CO_2	0.2175	0.2514	0.2514	0.2278	0.2278	0.2175	0.2175	0.0373	0.0000	0.0000	0.9999
Mole frac H_2	0.7462	0.7139	0.7139	0.6395	0.6395	0.7462	0.7462	0.0008	0.0009	0.0009	0.0000
Mole frac H_2O	0.0000	0.0000	0.0000	0.0474	0.0474	0.0000	0.0000	0.4775	0.5097	0.5097	0.0001
Mole frac CH_3OH	0.0053	0.0051	0.0051	0.0529	0.0529	0.0053	0.0053	0.4844	0.4894	0.4894	0.0000

	F-H2	H2-HP	H2-STRIP	HEAVIES	LIGHTS	LIQ	MEOH	PURGE	RX-IN	RX-OUT	VAP
Temperature C	35.0	170.0	47.0	104.9	39.0	30.0	39.0	30.0	225.0	250.0	30.0
Pressure bar	1.1	45	45	1.1	1.013	45	1.013	45	50	50	45
Vapor frac	1	1	1	0	1	0	0	1	1	1	1
Mole flow kmol/h	1190.00	1190.00	1213.51	407.56	1.04	3.48	390.43	0.01	9041.05	8259.03	1210.03
Mass flow kg/h	2658.87	2658.87	3985.80	7346.68	12.52	89.96	12508.71	0.10	122002.69	122002.69	3895.84
Volume flow cum/h	27734.24	992.69	735.89	8.05	26.70	0.11	16.12	0.00	7644.01	7304.78	695.46
Enthalpy gcal/h	−0.86	0.28	−3.13	−27.45	−0.02	−0.22	−22.11	0.00	−208.89	−212.71	−3.10
Mass flow kg/h											
CO	0.00	0.00	2.11	0.00	0.00	0.00	0.00	0.01	7492.57	7492.57	2.11
CO_2	0.00	0.00	1344.95	0.00	0.00	0.71	0.00	0.08	100018.93	82810.73	1344.24
H_2	2366.14	2366.14	2365.99	0.00	1.40	0.01	0.05	0.01	13011.73	10647.05	2365.99
H_2O	292.73	292.73	28.08	7336.52	0.00	27.66	1.20	0.00	4.80	7048.93	0.41
CH_3OH	0.00	0.00	244.67	10.16	11.12	61.58	12507.46	0.00	1474.66	14003.40	183.09
Mass frac CO	0.0000	0.0000	0.0005	0.0000	0.0000	0.0000	0.0000	0.0715	0.0614	0.0614	0.0005
Mass frac CO_2	0.0000	0.0000	0.3374	0.0000	0.0000	0.0079	0.0000	0.7902	0.8198	0.6788	0.3450
Mass frac H_2	0.8899	0.8899	0.5936	0.0000	0.1119	0.0001	0.0000	0.1242	0.1067	0.0873	0.6073
Mass frac H_2O	0.1101	0.1101	0.0070	0.9986	0.0000	0.3075	0.0001	0.0000	0.0000	0.0578	0.0001
Mass frac CH_3OH	0.0000	0.0000	0.0614	0.0014	0.8880	0.6846	0.9999	0.0141	0.0121	0.1148	0.0470
Mole frac CO	0.0000	0.0000	0.0001	0.0000	0.0000	0.0000	0.0000	0.0309	0.0296	0.0324	0.0001
Mole frac CO_2	0.0000	0.0000	0.0252	0.0000	0.0000	0.0046	0.0000	0.2175	0.2514	0.2278	0.0252
Mole frac H_2	0.9863	0.9863	0.9672	0.0000	0.6671	0.0009	0.0001	0.7462	0.7139	0.6395	0.9700
Mole frac H_2O	0.0137	0.0137	0.0013	0.9992	0.0000	0.4416	0.0002	0.0000	0.0000	0.0474	0.0000
Mole frac CH_3OH	0.0000	0.0000	0.0063	0.0008	0.3329	0.5528	0.9998	0.0053	0.0051	0.0529	0.0047

loading of 865 kg catalyst (Cu/Zn/Al/Zr). More catalyst could be added, but the improvements on the conversion are not significant since the operation under these conditions is practically equilibrium limited. A bed voidage (defined as the fraction of the reactor volume not occupied by catalyst) of 0.98 was used in simulations. This means that the fibrous Cu/Zn/Al/Zr catalyst reported in An et al. [2] is taken on a support and that 0.02 volume fraction (based on reactor) of active catalyst material is used.

The reactor outlet stream is cooled down in the FEHE unit and an additional Cooler, then being eventually flashed in a separator (Sep) to split methanol and water (liquid) from the non-condensable gas components (CO, CO_2 and H_2) that are recycled. The recycle stream is then purged (optionally, up to 1.5%) and mixed with the fresh CO_2 feed stream and sent to the second compressor (COMP2). The liquid stream of the flash is sent to a stripping column (STRIPPER) where the compressed wet hydrogen stream from COMP1 is fed in counter-current mode. This has a double positive effect, as it dries the hydrogen feed thus removing water from the reactor feed, and it removes the light ends (mainly CO_2 but CO as well) which are completely recycled thus significantly improving the consumption figures. The liquid bottom stream of the stripper is sent to a distillation column (DC) that separates water as bottom product and methanol as high purity top distillate. It is worth noting that by using the stripper unit, the liquid outlet (containing methanol–water) is obtained at higher temperature – the consequence of using a warmer feed stream to the DC unit being a reduced reboiler duty. Note that the separation of the methanol–water stream is carried out in a single distillation column using a partial condenser – able to deliver a vapor distillate (lights), high purity liquid distillate (methanol) and bottom product (water). Consequently, one distillation column (including reboiler and condenser) of the conventional direct sequence is spared. A dividing-wall column (DWC) can be also considered as an alternative for this ternary separation [12], in order to further reduce the (minor) methanol loss in the lights stream.

4.3. Consumption figures

For convenience, Table 7 gives the key parameters and consumption figures for this process. Remarkable, a large part of the

Table 7
Key performance indicators and consumption figures for the proposed process for methanol synthesis by CO_2 hydrogenation.

Parameter	Value	Unit
MeOH production rate	100.07	kton/year
Purge to feed ratio	0	mol/mol
Recycle to feed ratio	5.47	mol/mol
H_2:CO_2 ratio (feed/reactor inlet)	3.0/2.84	mol/mol
H_2 conversion in reactor (per pass)	18.17	%
CO_2 conversion (per pass)	17.20	%
MeOH yield (overall process)	99.83	%
Power of H_2 feed compressor (COMP1)	5962.96	kW
Power of recycle compressor (COMP2)	911.96	kW
Heat generated in the reactor	−4448.72	kW
Heat duty of reboiler (distillation column)	7618.42	kW
Electricity usage (per ton methanol)	550	kWh/ton MeOH
Steam usage (per ton methanol) – no heat integration	1.16	ton steam/ton MeOH
Steam usage (per ton methanol) – heat integrated[a]	0.48	ton steam/ton MeOH
Electricity cost (at 0.08 €/kWh)	49.37	Euro/ton MeOH
Steam cost (at 25 €/ton steam) – no heat integration	29.03	Euro/ton MeOH
Steam cost (at 25 €/ton steam) – heat integrated[a]	12.08	Euro/ton MeOH
Pure CO_2 use (per unit of methanol product)	1.3758	kg/kg
Pure H_2 use (per unit of methanol product)	0.1892	kg/kg
Wet H_2 use (per unit of methanol product)	0.2126	kg/kg

[a] *Note:* The heat integrated option means that part of the steam required in the reboiler of the distillation column is produced by using the heat generated in the reactor.

Table 8
Comparison of key performance indicators for two cases (without and with stripper) – as described in the patent of Kiss et al. [14].

Key performance indicators	Case A−	Case A+	Case B−	Case B+
CO_2 conversion per pass (%)	20.90	21.51	21.50	21.55
CO_2 conversion overall (%)	95.18	99.78	95.18	99.78
Electricity usage (kWh/ton MeOH)	607	588	597	581
Steam usage (ton steam/ton MeOH) – no HI	1.92	1.52	1.77	1.52
CO_2 use per unit of methanol product (kg/kg)	1.494	1.376	1.443	1.376
H_2 usage per unit of methanol product (kg/kg)	0.197	0.189	0.190	0.189

[a]*Note:* Case A: wet hydrogen feed. Case B: dry hydrogen feed. Both cases are considered without (−) or with (+) stripper. Operating conditions: P = 50 bar, T = 225 °C, H_2:CO_x = 6:1.

total reboiler duty (about 60%) can be covered by the thermal energy produced in the reactor, by generating high pressure steam usable in the reboiler. It is also worth noting that the consumption of raw materials is extremely close to the minimum stoichiometric value, while the use of utilities (steam and electricity) is also very low. The patent of Kiss et al. [14] includes several comparative examples showing that at various operating conditions this novel process using hydrogen stripping of products allows 15–20% energy savings and 5–8% more methanol product as compared to the conventional process. For convenience, Table 8 shows a comparison between two cases not limited by equilibrium (without and with stripper) as described in the patent of Kiss et al. [14] which provides more details about these cases and covers more possible process configurations. The advantages of using a stripping unit are clearly illustrated by the lower consumption figures, higher resource efficiency, as well as higher conversion of the raw materials.

5. Conclusions

The methanol synthesis by carbon dioxide hydrogenation is feasible in the new efficient process proposed here. A key feature of this novel process is the use of a stripping unit where the wet hydrogen (saturated with water) flows in counter-current with the condensed mixture methanol–water resulting from the flash separation after reaction. This operation has a double positive effect, as it removes CO_x from the methanol–water mixture thus allowing a complete recycle of CO_2, while also removing the water from the wet hydrogen (initially saturated with water) thus avoiding the negative impact on the reaction equilibrium conversion.

As a result, the consumption figures indicate a limited use of utilities (550 kWh/ton methanol, and 0.48–1.16 ton steam per ton methanol) while the use of the raw materials is minimal, as both reactants are recovered and recycled hence completely converted in the overall process – being limited by the stoichiometry only. While all the carbon from the CO_2 feed ends up in the methanol product, the hydrogen valorization is less efficient since only two thirds of hydrogen is converted to methanol product, the rest being converted to the water by-product.

References

[1] K.A. Ali, A.Z. Abdullah, A.R. Mohamed, Recent development in catalytic technologies for methanol synthesis from renewable sources: a critical review, Renew. Sustain. Energy Rev. 44 (2015) 505–518.
[2] X. An, Y. Zuo, Q. Zhang, J. Wang, Methanol synthesis from CO_2 hydrogenation with a Cu/Zn/Al/Zr fibrous catalyst, Chin. J. Chem. Eng. 17 (2009) 88–94.
[3] A.N.R. Bos, P.C. Borman, M. Kuczynski, K.R. Westerterp, The kinetics of the methanol synthesis on a copper catalyst: an experimental study, Chem. Eng. Sci. 44 (1989) 2435–2449.
[4] G. Centi, S. Perathoner, Opportunities and prospects in the chemical recycling of carbon dioxide to fuels, Catal. Today 148 (2009) 191–205.
[5] A. Coteron, A.N. Hayhurst, Kinetics of the synthesis of methanol from CO + H_2 and CO + CO_2 + H_2 over copper-based amorphous catalysts, Chem. Eng. Sci. 49 (1994) 209–221.
[6] A.C. Dimian, C.S. Bildea, A.A. Kiss, Integrated Design and Simulation of Chemical Processes, second ed., Elsevier, Amsterdam, 2014.
[7] E. Fiedler, G. Grossmann, D.B. Kersebohm, G. Weiss, C. Witte, Methanol, in Ullmann's Encyclopedia of Industrial Chemistry, Wiley-VCH, 2005.
[8] G.H. Graaf, P.J.J.M. Sijtsema, E.J. Stamhuis, G.E.H. Joosten, Chemical equilibria in methanol synthesis, Chem. Eng. Sci. 41 (1986) 2883–2890.
[9] G.H. Graaf, E.J. Stamhuis, A.A.C.M. Beenackers, Kinetics of low-pressure methanol synthesis, Chem. Eng. Sci. 43 (1988) 3185–3195.

[10] S.G. Jadhav, P.D. Vaidya, B.M. Bhanage, J.B. Joshi, Catalytic carbon dioxide hydro-genation to methanol: a review of recent studies, Chem. Eng. Res. Des. 92 (2014) 2557–2567.
[11] A.A. Kiss, Process Design and Control by Nonlinear Analysis: Applications to Reactor-separator-Recycle systems, Lambert Academic Publishing, Cologne, Germany, 2010.
[12] A.A. Kiss, Advanced Distillation Technologies – Design, Control and Applications, Wiley, Chichester, UK, 2013.
[13] A.A. Kiss, C.S. Bildea, A.C. Dimian, Design and control of recycle systems by non-linear analysis, Comput. Chem. Eng. 31 (2007) 601–611.
[14] A.A. Kiss, J.J. Pragt, M.M. van Iersel, G. Bargeman, M.T. de Groot, Continuous process for the preparation of methanol by hydrogenation of carbon dioxide, Patent No. WO/2013/144041 (EP-2831025), 2013.
[15] E.V. Kondratenko, G. Mul, J. Baltrusaitis, G.O. Larrazábal, J. Pérez-Ramírez, Status and perspectives of CO_2 conversion into fuels and chemicals by catalytic, photocatalytic and electrocatalytic processes, Energy Environ. Sci. 6 (2013) 3112–3135.
[16] H.W. Lim, M.J. Park, S.H. Kang, H.J. Chae, J.W. Bae, K.W. Jun, Modeling of the kinetics for methanol synthesis using $Cu/ZnO/Al_2O_3/ZrO_2$ catalyst: influence of carbon dioxide during hydrogenation, Ind. Eng. Chem. Res. 48 (2009) 10448–10455.
[17] X.-M. Liu, G.Q. Lu, Z.-F. Yan, J. Beltramini, Recent advances in catalysts for methanol synthesis via hydrogenation of CO and CO_2, Ind. Eng. Chem. Res. 42 (2003) 6518–6530.
[18] G.A. Olah, A. Goeppert, G.K. Surya Prakash, Beyond Oil and Gas – The Methanol Economy, second ed., Wiley-VCH, Weinheim, Germany, 2009.
[19] S. Saeidi, N.A.S. Amin, M.R. Rahimpour, Hydrogenation of CO_2 to value-added products – a review and potential future developments, J. CO_2 Utilization 5 (2014) 66–81.
[20] K.M. Vanden Bussche, G.F. Froment, A steady-state kinetic model for methanol synthesis and the water gas shift reaction on a commercial $Cu/ZnO/Al_2O_3$ catalyst, J. Catalysis 161 (1996) 1–10.
[21] X. Yan, H. Guo, D. Yang, S. Qiu, X. Yao, Catalytic hydrogenation of carbon dioxide to fuels, Curr. Org. Chem. 18 (2014) 1335–1345.